SUPPLEMENTAL DATA

Control of yeast filamentous-form growth by modules in an integrated molecular network

Susanne Prinz[1], Iliana Avila-Campillo[1], Christine Aldridge[1], Ajitha Srinivasan[1], Krassen Dimitrov[1], Andrew F. Siegel[1,2], and Timothy Galitski[1,3]

[1] Institute for Systems Biology, 1441 N. 34th Street, Seattle, WA 98103

[2] University of Washington, Departments of Management Science, Finance, and Statistics, Seattle WA 98195

[3] Corresponding author, tgalitski@systemsbiology.org

Efficiency of yeast differentiation to the filamentous form

The efficiency and robustness of differentiation to the filamentous form was tested using a strain with a fusion of the *FLO11* promoter to the coding sequence of Green Fluorescent Protein (GFP). The *FLO11* gene is induced during filamentous growth (Rupp et al. 1999). Cells collected after several hours on SLAD plates show filamentous morphology (Supplemental Figure 1A) and induction of *FLO11* expression (Supplemental Figure 1B). Supplemental Figure 1C shows distributions of GFP fluorescence for yeast-form cells and filamentous-form cells incubated for 10 hours on SLAD. The filamentous-form cell population shows a single-peak distribution of fluorescence in which almost all cells have more fluorescence than the average fluorescence of yeast-form cells.

For studies of *FLO11::GFP* expression, cells were prepared as described for expression profiling (Methods). In addition, filaments of attached cells were dissociated into single cells by shearing (Kron et al. 1994). Microscopy with methylene-blue staining verified that the cells were separated, intact, and viable. Fluorescence microscopy was done with a Zeiss Axiophot microscope with a 100X objective. Fluorescence images were captured using RS Image software from Roper Scientific. Fluorescence distributions in cell populations were measured by fluorescence-activated cell sorting analysis, using a Becton Dickinson FACScalibur flow cytometer.

Assembly of global protein-protein and protein-metabolite interaction networks

A global protein-protein interaction network was assembled from various published

sources. This global network served as the source for protein-protein interactions in the filamentation network. Yeast protein-protein interactions were compiled from the Munich Information Center for Protein Sequences database (http://mips.gsf.de) (Mewes et al. 2000), the Biomolecular Interaction Network Database (http://www.bind.ca) (Bader et al. 2003), a global two-hybrid screen (Ito et al. 2001), and a composite dataset (Schwikowski et al. 2000). Self interactions were removed. Based on the work of Rives and Galitski (2003) and Steffen et al. (2002) the interactions of 15 high-connectivity proteins were removed. The final global protein-protein network has 5614 interactions and 3755 proteins.

From the yeast metabolic network compiled by Forster et al. (2003), interactions between protein-enzymes and their metabolite substrates/products were extracted. The metabolic interactions of the 27 highest-connectivity metabolic nodes (e.g., ATP) were removed. The resulting metabolic network contains 2098 protein-metabolite interactions among 779 metabolites and 561 protein-enzymes.

Non-random interaction among filamentation proteins

Our assembly and analysis of an integrated network restricted to filamentation proteins and the interaction paths among them (rather than a global network; see Results) was motivated by the desire to focus on a network that is available and active in filamentous growth. The advantages of this approach presume a non-random tendency to interact among the filamentation proteins. This presumption predicts that either randomized interaction data, or random substitutes for the filamentation genes, will result in a relatively sparse integrated restricted network that has fewer interactions and fewer

incident edges per node (mean node degree) than the biological filamentation network. The first three data rows of Supplemental Table 2 confirm this prediction. One possible interpretation of these data is that the phenotype-implicated proteins (identified by a database query) have been foci of intensive research, therefore they share many validated interactions. The analysis was repeated for a network that contains only the expression-implicated proteins, the vast majority of which have not been reported to be filamentation proteins. The resulting data (Supplemental Table 2, last three rows) show essentially the same result, indicating that it does not depend on the intensively studied phenotype-implicated proteins.

Network clustering method

The integrated filamentation network was clustered using the method of Rives and Galitski (2003) modified and extended as follows. Briefly, graph nodes are clustered using average-linkage agglomerative hierarchical clustering in which the distance metric is the Manhattan distance between the all-pairs-shortest-paths (APSP) distance profiles of nodes.

Typical application of hierarchical clustering leaves the exact boundaries of clusters to interpretation. We extended network clustering by computing explicit cluster boundaries. A minimum size for a network cluster was set at 3 joined protein nodes. Supplemental Figure 2A shows a plot of number of clusters as a function of join number (iteration of the hierarchical clustering algorithm). With successive joins, new clusters are formed and nodes are added to existing clusters. Late in the clustering, most joins result in the fusion of existing clusters. This phase corresponds to a rapid increase in the

distance metric (Supplemental Figure 2B), indicating the joining of graph elements with increasingly different APSP profiles. This suggests that joins preceding this terminal phase best reflect the clustered structure of the network. To specify cluster membership, the highest join number with the highest number of clusters was identified. This join occurs between the cluster formation phase and the terminal cluster-fusion phase. For the filamentation network, this was the 535th join (arrows in Supplemental Figure 2), specifying the membership of 47 clusters. For other integrated biomolecular networks, similar patterns of cluster number and distance were observed (unpublished data).

At each iteration of hierarchical clustering, only clusters that are adjacent in the network are candidates for joining. In addition to decreasing run time, this constraint precludes joining nonadjacent molecules/clusters that have low Manhattan distances due to network symmetries resulting in similar profiles of distances to other nodes. With continued clustering, these symmetrically located elements become adjacent and are clustered at later joins with lower distances. This is illustrated by the non-monotonicity of the distance plot in Supplemental Figure 2B. Each cluster was assigned the name of the member node of highest intracluster degree (number of connections to cluster co-members). Ties were broken using the following priorities from highest to lowest: proteins with common names, metabolites, proteins with no common name, highest total degree, and random selection.

The methods were implemented in Java and incorporated as the *Biomodules* plug-in to the *Cytoscape* open-source software platform (http://www.cytoscape.org) (Shannon et al. 2003) for biomolecular network integration, visualization, and analysis. *Biomodules* source code can be obtained at http://labs.systemsbiology.net/galitski . In addition, one

can use *Biomodules* at http://labs.systemsbiology.net/galitski . Neither data upload nor software download is required to use *Biomodules*. The only requirement is installation of Java Web Start or Java 1.4.1 or higher (Sun Microsystems, http://java.sun.com).

Analysis of expression-change co-ordination of cluster co-members

To test for significant expression-change coordination among network-cluster co-member genes, a null hypothesis was evaluated. The null hypothesis states that the induced genes, repressed genes, and genes not-significantly-changed are randomly distributed among the network clusters. For purposes of this analysis, the clusters of the filamentation network contain 141 classes of genes (induced, repressed, and not-significantly-changed, distributed in 47 clusters, 47 x 3 = 141). Each class has an observed and an expected frequency. The expected frequencies are based on the null hypothesis of random assortment of the induced, repressed, and not-significantly-changed proteins among the 47 clusters. The 141 classes are constrained by 48 sums, leaving 93 degrees of freedom. One sum constrains the total number of proteins, and 47 sums constrain the number of proteins in the clusters. A likelihood-ratio test (Sokal and Rohlf 1995) results in G=214, with 93 degrees of freedom, $p=10^{-11}$, and rejection of the null hypothesis.

Because the number of genes expected in each of the 141 classes is rather low, there was the possibility of a low p-value due to sample bias. To further test the null hypothesis, genes were randomly reassigned to the clusters, preserving the number of clusters and number of gene members of each cluster. In 10000 independent tests, G=113±14 (mean±sd) and G_{max}=165 were observed. Because the value of G observed for the biological data (G=214) is significantly higher than the distribution observed in these

random trials with the same network constraints, the rejection of the null hypothesis was confirmed.

Not all clusters contribute equally to the finding of expression-change coordination. Supplemental Table 4 provides cluster-specific information on non-random expression change. The table lists, for each cluster, the total number of genes, the number of genes induced, repressed, and not-changed, as well as the contribution of each cluster to the *G* statistic of the likelihood-ratio test. The overall *G* is the sum of the *G*s for the various clusters. A higher *G* indicates greater discrepancy between the observed data and the data expected based on the null hypothesis.

Analysis of cluster-annotation significance

To test for collective function among cluster co-members, over-represented gene annotations, including significance values, were assigned to clusters (Table 1 in the main text). It was possible that these results were due to multiple hypothesis testing, because Table 1 reports the annotation of highest significance among many annotations that were examined. Note, however, that these multiple hypotheses (annotations) are not independent. Nonetheless, to calibrate the results of Table 1, networks with randomized gene assignments were analyzed. Genes were randomly reassigned to clusters and the numbers of genes in each cluster were preserved. For 30 independent randomizations, the analysis in Table 1 was repeated, except that no p-value cutoff was applied. The highest $-\log_{10}$p-values for each cluster were binned in a histogram. Supplemental Figure 3A shows a p-value histogram representing the averages from the 30 randomizations. Supplemental Figure 3B shows the p-value histogram representing the filamentation

network. The results confirm the significance of cluster collective functions in the filamentation network and allow estimation of false-discovery rates for varying p-values.

Peroxisome proliferation in filamentous-form cells

The emergence of the **DAL2** and **POX1** modules led to insights on filamentous-form cell biology. In yeast-form cells growing with plentiful glucose and ammonium, cells with detectable peroxisomes are scarce. Growth on oleic acid as a carbon source induces the proliferation of peroxisomes in most cells (Veenhuis et al. 1987). The filamentous-form induction of metabolic pathways known to be housed in peroxisomes suggested that peroxisomes proliferate in filamenting cells. To test this, cells were transformed with plasmid pDsRed-PTS1, encoding a DsRed fluorescent protein with a peroxisomal-localization signal peptide. This results in fluorescent peroxisomes, if they are present. Yeast-form and filamentous-form cells were compared. Peroxisomes proliferate in filamentous-form cells (Supplemental Figure 4). About 5% of yeast-form cells showed some peroxisomal fluorescence. On SLAD plates with plentiful glucose and no added fatty acids, the frequency of cells showing punctate fluorescence increases to about 20% at 10 hours and 50% at 3 days of incubation. It was possible that the observed fluorescent foci were agglomerates of DsRed protein. This possibility was excluded by testing an isogenic peroxisome-deficient *pex3D* mutant. In this mutant no DsRed foci were observed (Supplemental Figure 4). Proliferation of peroxisomes also was observed using a different fluorescent peroxisome reporter (data not shown), pPTS2-GFP.

Yeast cells transformed with plasmid pDsRed-PTS1 or plasmid pPTS2-GFP (kindly provided by J. Smith and J. Aitchison) (Smith et al. 2002) were grown for 10

hours on either SLAD or SCD (plentiful glucose and ammonium) agar. Cells were washed off plates with the respective liquid medium and inspected for punctate fluorescence using a Leica confocal microscope. At least 100 cells per strain and condition were observed and scored.

SUPPLEMENTAL FIGURE LEGENDS

Supplemental Figure 1. Efficient differentiation of yeast cell populations. Yeast cells with a fluorescent filamentation-expression reporter, *FLO11::GFP::kanMX6::FLO11+*, were grown for several hours on SLAD plates, collected and imaged by (A) phase-contrast microscopy and (B) fluorescence microscopy. (C) The distribution of fluorescence (on a logarithmic axis) in *FLO11::GFP::kanMX6::FLO11+* cells. Cell populations from yeast-form and filamentous-form growth conditions were analyzed.

Supplemental Figure 2. Quantitative identification of network clusters. The nodes of the filamentation network were iteratively joined into clusters (see text). (A) A cluster was defined as a joined group containing at least 3 protein nodes. The number of clusters is plotted as a function of join number. (B) The selection of nodes/clusters to join was based on average-linkage Manhattan distance of node shortest-paths-distance profiles. This distance metric is plotted as a function of join number. In both (A) and (B) the arrow indicates the 535^{th} join, corresponding to the highest join number with the highest number of clusters. Clustering of the filamentation network was terminated at this join iteration.

Supplemental Figure 3. Significance distributions of cluster annotations. The highest $-\log_{10}$p-values for each network cluster were binned in a histogram. (A) The significance distribution of network clusters with random gene reassignments (means, n=30). (B) The significance distribution of filamentation-network clusters.

Supplemental Figure 4. Peroxisome proliferation during filamentous growth. All strains harbor a plasmid expressing a peroxisome-localized fluorescent protein, DsRed-PTS1. Localization of DsRed-PTS1 was analyzed by confocal fluorescence microscopy. (A) Wild type and *pex3D* were grown on SLAD agar plates for 10 hours. (B) Wild type was grown on SCD agar for 10 hours.

SUPPLEMENTAL FIGURE 1

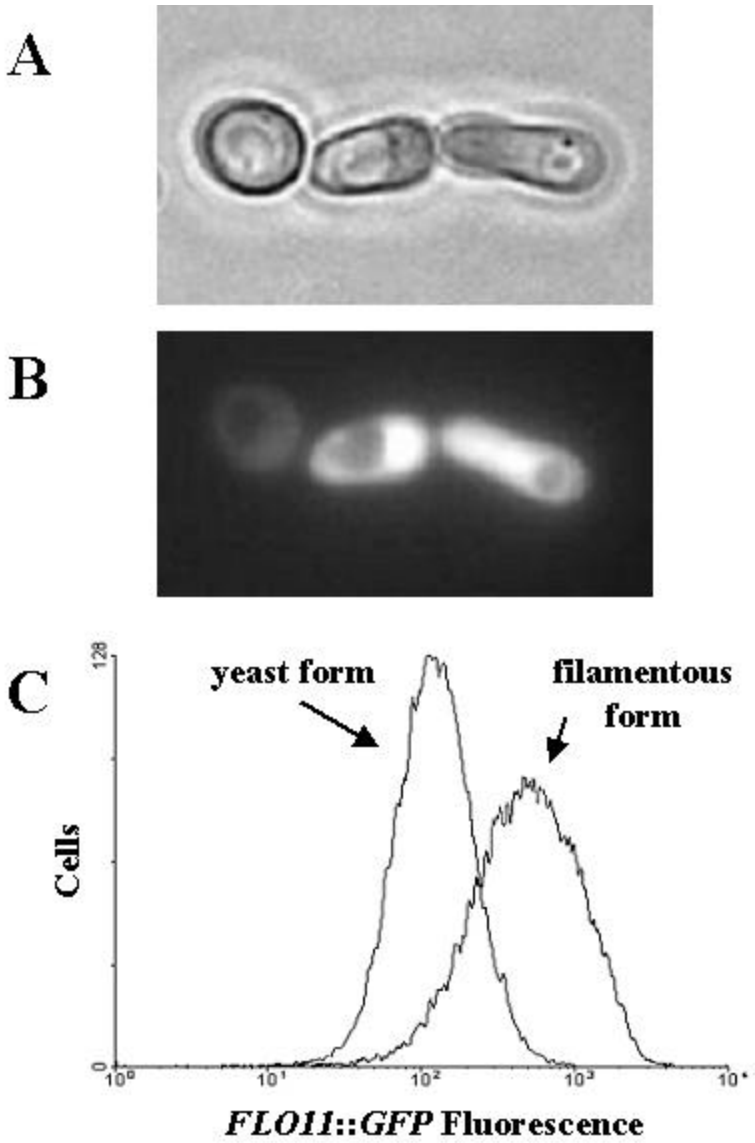

SUPPLEMENTAL FIGURE 2

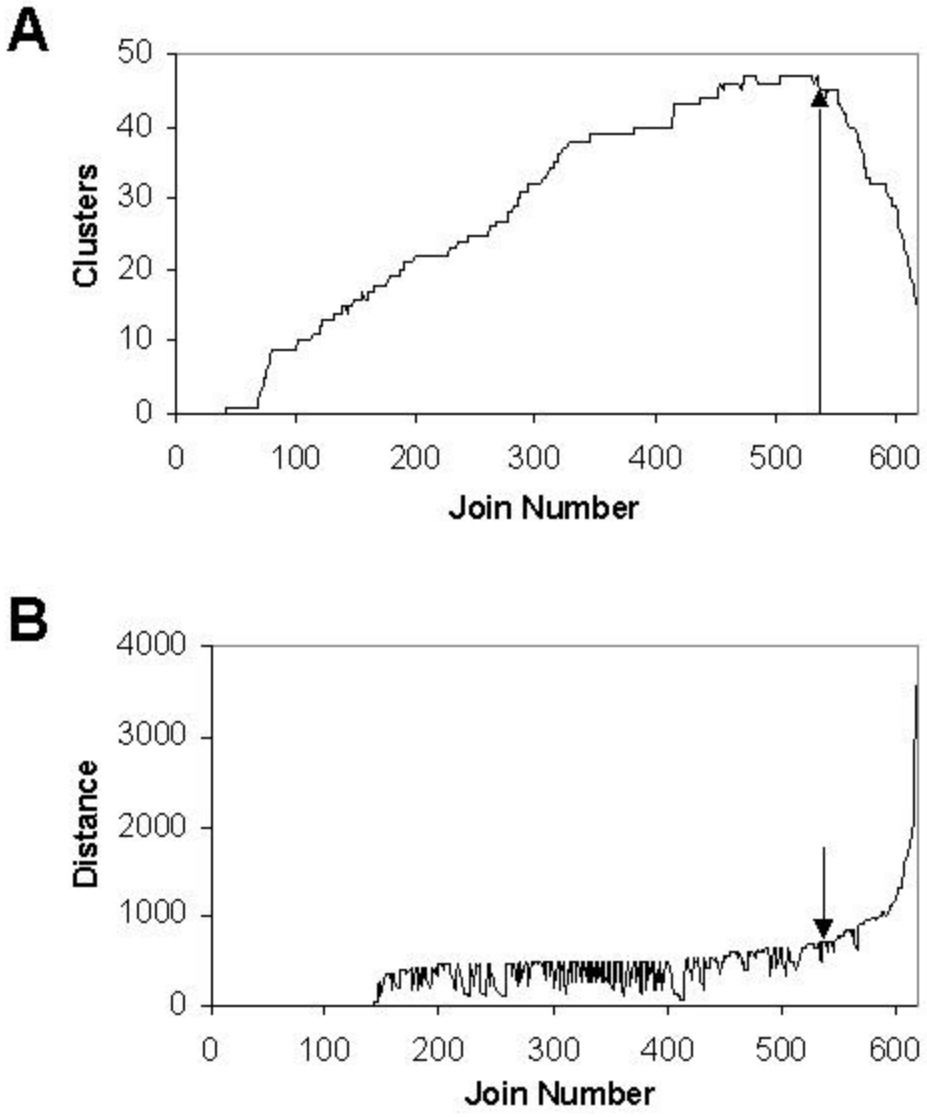

SUPPLEMENTAL FIGURE 3

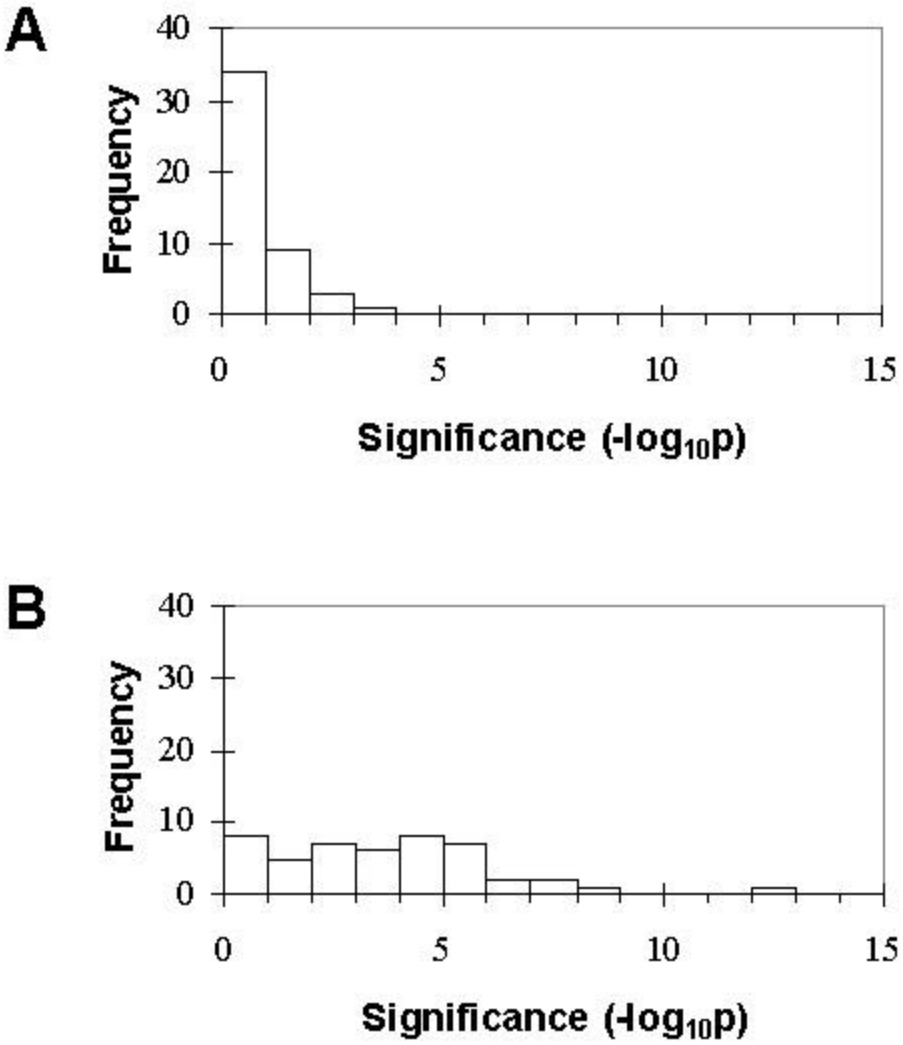

SUPPLEMENTAL FIGURE 4

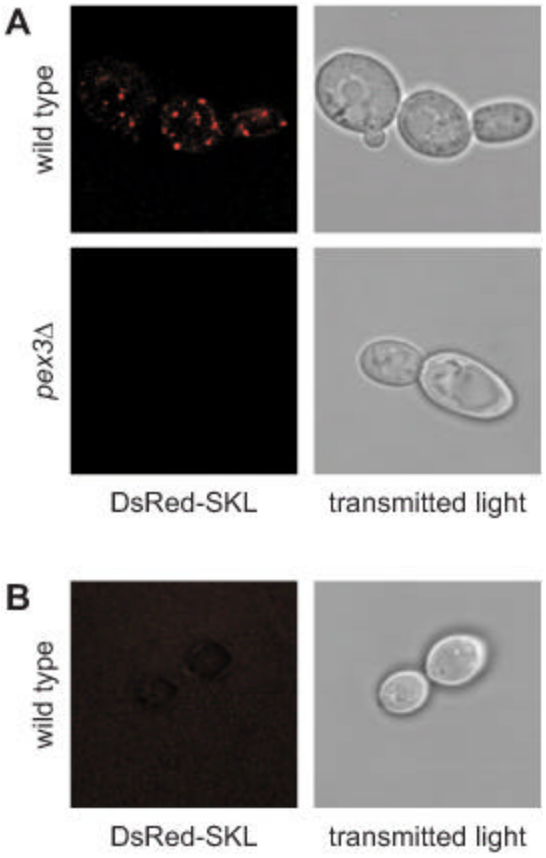

SUPPLEMENTAL TABLES

Supplemental Table 1. Filamentous-form/yeast-form expression ratios

See accompanying file, Prinz_SuppleTable1.txt

Supplemental Table 2. Non-random interaction among filamentation proteins

		Network		
Interaction data [a]	**Protein list** [b]	**Interacting proteins** [c]	**Interactions** [d]	**Mean node degree** [e]
biological	filamentation 1026	380	534	2.8
biological	random 1026	388±13	289±14	1.5±0.1
random	filamentation 1026	265±20	266±41	2.0±0.3
biological	expression 873	269	396	2.9
biological	random 873	206±16	188±18	1.8±0.2
random	expression 873	276±16	192±17	1.4±0.1

[a] Interaction data include all protein-protein interactions plus all metabolic interactions (proteins interacting via a metabolite). Each analysis used either biological interaction data or 10 data sets in which interactions were reassigned randomly to pairs of proteins.

[b] Each analysis included a list of either the 1026 filamentation proteins, or the 873 expression-implicated proteins, or 10 sets of random proteins.

[c] The number (mean±sd) of proteins in the list that has at least one interaction with another protein in the list.

[d] The number (mean±sd) of direct interactions between pairs of proteins in the list.

[e] Node degree is the number of incident edges of the node. Mean node degree is the ratio of twice the number of interactions to the number of interacting proteins.

Supplemental Table 3. Components of filamentation-network clusters

Cluster components
ACP1
ACP1, NADHM, IDP1, ALD4, UbiquinolM, Ubiquinone-9M, MET13, IDH1, IDH2, NADPHM, NADP+M, PUT1, ADH3, 2-OxoglutarateM, IsocitrateM, COX8, COX7, SDH4, COX5A, AcetaldehydeM, PPA1, (S)-1-Pyrroline-5-carboxylateM, Malonyl-[acyl-carrier protein]M, 5,10-MethylenetetrahydrofolateM, Dodecanoyl-[acyl-carrier protein]M, Palmitoyl-[acyl-carrier protein]M, Decanoyl-[acyl-carrier protein]M, Oleoyl-[acyl-carrier protein]M, Stearoyl-[acyl-carrier protein]M, Myristoyl-[acyl-carrier protein]M, EthanolM, L-ProlineM, OxalosuccinateM, Hexadecanoyl-[acp]M, Linolenoyl-[acyl-carrier protein]M, Acyl-carrier proteinM, Acyl-[acyl-carrier protein]M, 5-MethyltetrahydrofolateM, Tetradecenoyl-[acyl-carrier protein]M

STE11

KSS1, *STE11*, *DIG1*, *STE4*, *STE7*, *AKR1*, *STE12*, *DIG2*, *SPA2*, *STE50*, *HSC82*, *SPH1*, STI1, *MPT5*, *PEA2*, MRP5, *WHI2*, *RAS1*, *HOG1*, YEL048C

CDC28

CDC28, *CLB2*, *CLN2*, SWI4, *CLN3*, *YDJ1*, *CDC6*, *CAK1*, *HSL1*, *CLN1*, SSB1, MUS81, *CLB1*

POX1

POX1, Acetyl-CoA, OSM1, GNA1, ERG13, DAL7, MLS1, Malate, FUM1, CIT2, FADM, (S)-3-Hydroxy-3-methylglutaryl-CoA, Glyoxylate, FADH2M, FumarateM, HMG1, SuccinateM, Palmitate, Citrate, Myristic acid, D-Glucosamine 6-phosphate, N-Acetyl-D-glucosamine 6-phosphate, Acetoacetyl-CoA, Stearate

ACT1

CDC42, *ACT1*, GLK1, *BEM1*, *STE20*, *BUD6*, *BNI1*, alpha-D-Mannose, *BMH2*, *PGI1*, BOI2, beta-D-Glucose 6-phosphate, alpha-D-Glucose 6-phosphate, *BEM4*, *CLA4*, *SLA2*, HXT1, *SHO1*, *BMH1*, *FIG1*, COF1, *GIC1*, *RSR1*, GIC2, BOP3, HXT2, ATC1, D-Mannose 6-phosphate, beta-D-Glucose, YGL015C

BNA6

BNA6, KAP95, RIB4, GSP1, *MSN5*, *YAP1*, *PSE1*, *SWI5*, THI4, 5-Phospho-alpha-D-ribose 1-diphosphateM, Nicotinate D-ribonucleotideM, Pyridine-2,3-dicarboxylate, 5-Amino-6-ribitylamino-2,4 (1H, 3H)-pyrimidinedione, Nicotinate D-ribonucleotide, 5-Phospho-alpha-D-ribose 1-diphosphate, PyrophosphateM, CO2M, L-3,4-Dihydroxy-2-butanone 4-phosphate, Pyridine-2,3-dicarboxylateM, 6,7-Dimethyl-8-(1-D-ribityl)lumazine

PDE2

PDE2, CHO1, CMP, CPT1, PIS1, EPT1, Diacylglycerol, myo-Inositol, CDPdiacylglycerol, 1-Phosphatidyl-D-myo-inositol, ITR1, IPT1, *PLC1*, 3',5'-Cyclic dAMP, Phosphatidylcholine, L-Serine, 3',5'-Cyclic AMP, CMPM, L-SerineM, CDPethanolamine, 3',5'-Cyclic IMP, CDPcholine, dAMP, CDPdiacylglycerolM, 3',5'-Cyclic GMP, 3',5'-Cyclic CMP, GMP, PhosphatidylserineM, Phosphatidylserine, IMP, Phosphatidylethanolamine

BAP2

BAP2, MET6, L-Methionine, MUP3, HNM1, L-MethionineX, Homocysteine, L-Tryptophan, YFR055W, EFT1, BNA2, CholineX, Tetrahydropteroyltri-L-glutamate, Prephenate, L-Isoleucine, L-TyrosineX, L-IsoleucineX, L-CysteineX, L-Cysteine, L-Valine, L-ValineX, 5-Methyltetrahydropteroyltri-L-glutamate, L-Cystathionine, L-LeucineX, L-PhenylalanineX, L-Leucine, L-TryptophanX

GRR1

GRR1, YLR128W, *CDC53*, *DFG5*, YPR158W-B, YNL247W, YPR158W

RPP1B

RPP1B, RPP1A, TRX2, RPP0, PBI2, PEX2, *MGM101*

YIP1

YIP1, YIF1, YOP1, YIP3, YIP4, YLR324W, GAS3

AAH1

AAH1, FCY22, FCY2, Adenine, Cytosine, GuanineX, AdenineX, Guanine, CytosineX, YJL070C, BTN2, *RPB7*, Deoxyinosine, Deoxyadenosine, Hypoxanthine, Inosine

ADE5,7

ADE5,7, PIN3, UBI4, YBR101C, DDR48, *EGT2*, 2-(Formamido)-N1-(5'-phosphoribosyl)acetamidine, 5-Phosphoribosylamine, 5'-Phosphoribosylglycinamide, Aminoimidazole ribotide

ACAL

Acetaldehyde, PDC5, PDC1, *ADH1*, ALD6, Pyruvate, BDP1, Ethanol, YOR390W

BCY1

BCY1, *TPK2*, *SFL1*, *TPK1*, *TPK3*, YHR083W

ERG11

ERG11, Oxygen, URA1, ERG5, ERG3, ERG1, Ergosta-5,7,24(28)-trienol, Reduced flavoprotein, Episterol, Squalene, (S)-Dihydroorotate, Ergosta-5,7,22,24(28)-tetraenol, H2O2, (S)-2,3-Epoxysqualene, 4,4-Dimethylcholesta-8,14,24-trienol, Lanosterol, Oxidized flavoprotein

ACS1

ACS1, Acetyl-CoAM, CoAM, YAT1, CIT1, SRB2, IMH1, AcetateM

SNF1

SNF1, *SNF4*, SPT2, *SIP4*, YMR291W

DIP5

DIP5, ARG1, L-Aspartate, GLY1, ASP3-1, L-Asparagine, Glycine, L-GlutamateX, L-AsparagineX, GlycineX, N-(L-Arginino)succinate, L-Citrulline, L-AspartateX, L-Alanine, L-GlutamineX, L-SerineX, L-AlanineX, L-Threonine

ILV2

ILV2, ARG8, PyruvateM, YLR089C, GlutamateM, CYB2, N-Acetyl-L-glutamate 5-semialdehydeM, 2-Aceto-2-hydroxy butyrateM, 2-AcetolactateM, N2-Acetyl-L-ornithineM, 2-OxobutanoateM, L-AlanineM

13PDG

3-Phospho-D-glyceroyl phosphate, TDH2, TDH3, TDH1, YML053C

NH3xt

NH3xt, *MEP3*, *MEP2*, *MEP1*, TIP1

HSL7

SWI1, *HSL7*, *SWE1*, MUD2

YBL101W-A

YBL101W-A, YFL002W-A, YJL162C, YCL020W

YDR261W-A

YDR261W-A, YDR261W-B, YCL019W, YFL002W-B

YPR158W-A

YPR158W-A, YOR142W-A, YOL103W-B, YER159C-A

DAL2

DAL2, DAL4, DAL1, Allantoin, Allantoate, (-)-Ureidoglycolate, AllantoinX, Urea

MET17

MET17, Acetate, CDA1, ACH1, Chitosan, O-Acetyl-L-homoserine, Hydrogen sulfide, Methanethiol

CHS1

CHS1, CHS2, ACO1, UDP, Chitin, UDP-N-acetyl-D-galactosamine, CitrateM

ERG6

ERG6, S-Adenosyl-L-methionine, S-Adenosyl-L-homocysteine, SAH1, SAM1, Fecosterol, Zymosterol

AAT2

AAT2, ARO8, 3-(4-Hydroxyphenyl)pyruvate, L-Tyrosine, Oxaloacetate, PYC1

PMT2

PMT2, PMT1, PMT4, Dolichyl beta-D-mannosyl phosphate, Mannan, Dolichyl phosphate

CAP

Carbamoyl phosphate, ARG3, CPA1, CPA2, L-Ornithine

GDPMAN

GDPmannose, CSG2, DPM1, KTR1, Inositol phosphorylceramide

SPH

Sphinganine, SUR2, LCB3, YSR3, Phytosphingosine

AGA2

AGA2, *AGA1*, YGR257C

APP2

APP2, PEX21, RVS167

FKH1

FKH1, *RIM101*, YDR279W

FTR1

FTR1, FET3, YIL056W

GTR1

GTR1, GTR2, YJL097W

HMLALPHA2

HMLALPHA2, *TUP1*, *HMRA1*

MGA1

MGA1, TOS1, MRP4

PMA1

PMA1, PMP2, PMP1

RAD51

RAD51, APC2, *HRR25*

RPN12

RPN12, DON1, RPN4

SXM1

SXM1, RPL31B, RPL16B

TOM7

TOM70, TOM40, TOM7

For each cluster, molecular components are listed in order of intracluster degree, the number of interactions with other members of the same cluster, from highest to lowest. Protein components are all-capitalized and underlined; other components are metabolites. Mitochondrial pools of metabolites are indicated with a terminal “M”. A terminal “X” or “xt” indicates extracellular pools of metabolites. Proteins encoded by genes implicated by

a mutant filamentation-related phenotype are italicized. Proteins encoded by genes whose mRNA levels differ significantly between yeast-form cells and the filamentous form are colored. Red indicates higher expression in the filamentous form relative to the yeast form; blue indicates lower expression in the filamentous form.

Supplemental Table 4. Expression change within clusters

	Genes				
Cluster	**Total**	**Induced**	**Repressed**	**Unchanged**	*G*
STE11	20	4	2	14	19.7
CDC28	13	2	2	9	11.9
BCY1	6	1	0	5	10.9
ERG11	5	0	5	0	9.4
POX1	9	7	2	0	8.1
YDR261W-A	4	4	0	0	7.9
ILV2	4	4	0	0	7.9
YPR158W-A	4	4	0	0	7.9
YIP1	7	1	6	0	7.5
ACP1	13	7	6	0	7.3
RPN12	3	3	0	0	6.0
CAP	3	3	0	0	6.0
DAL2	3	3	0	0	6.0
AAT2	3	3	0	0	6.0

SNF1	5	2	0	3	5.8
SPH	3	0	3	0	5.7
PMA1	3	0	3	0	5.7
GDPMAN	3	0	3	0	5.7
PMT2	3	0	3	0	5.7
BAP2	7	2	5	0	5.0
ACT1	25	7	7	11	4.8
ACS1	5	1	4	0	4.5
PDE2	8	1	6	1	4.4
HMLALPHA2	3	1	0	2	3.9
FKH1	3	0	1	2	3.8
YBL101W-A	4	3	1	0	3.3
13PDG	4	1	3	0	3.1
MGA1	3	0	2	1	2.8
AGA2	3	0	2	1	2.8
GTR1	3	0	2	1	2.8
ADE5,7	6	4	1	1	2.3
DIP5	4	2	2	0	2.2
TOM7	3	2	1	0	2.0
MET17	3	2	1	0	2.0
APP2	3	2	1	0	2.0
SXM1	3	2	1	0	2.0
FTR1	3	1	2	0	1.9

ERG6	3	1	2	0	1.9
CHS1	3	1	2	0	1.9
HSL7	4	1	1	2	1.3
RPP1B	7	2	4	1	1.0
NH3xt	4	2	1	1	0.4
AAH1	6	2	3	1	0.3
ACAL	6	2	3	1	0.3
GRR1	7	2	3	2	0.2
RAD51	3	1	1	1	0.1
BNA6	9	3	4	2	0.1
SUM	**259**	**96**	**101**	**62**	**214.3**

SUPPLEMENTAL REFERENCES

Bader, G.D., Betel, D., and Hogue, C.W. 2003. BIND: the Biomolecular Interaction Network Database. *Nucleic Acids Res* **31**: 248-250.

Forster, J., Famili, I., Fu, P., Palsson, B.O., and Nielsen, J. 2003. Genome-scale reconstruction of the Saccharomyces cerevisiae metabolic network. *Genome Res* **13**: 244-253.

Ito, T., Chiba, T., Ozawa, R., Yoshida, M., Hattori, M., and Sakaki, Y. 2001. A comprehensive two-hybrid analysis to explore the yeast protein interactome. *Proc Natl Acad Sci U S A* **98**: 4569-4574.

Kron, S.J., Styles, C.A., and Fink, G.R. 1994. Symmetric cell division in pseudohyphae of the yeast Saccharomyces cerevisiae. *Mol Biol Cell* **5**: 1003-1022.

Mewes, H.W., Frishman, D., Gruber, C., Geier, B., Haase, D., Kaps, A., Lemcke, K., Mannhaupt, G., Pfeiffer, F., Schuller, C. et al. 2000. MIPS: a database for genomes and protein sequences. *Nucleic Acids Res* **28**: 37-40.

Rives, A.W. and Galitski, T. 2003. Modular organization of cellular networks. *Proc Natl Acad Sci U S A* **100**: 1128-1133.

Rupp, S., Summers, E., Lo, H.J., Madhani, H., and Fink, G. 1999. MAP kinase and cAMP filamentation signaling pathways converge on the unusually large promoter of the yeast FLO11 gene. *Embo J* **18**: 1257-1269.

Schwikowski, B., Uetz, P., and Fields, S. 2000. A network of protein-protein interactions in yeast. *Nat Biotechnol* **18**: 1257-1261.

Shannon, P., Markiel, A., Ozier, O., Baliga, N.S., Wang, J.T., Ramage, D., Amin, N., Schwikowski, B., and Ideker, T. 2003. Cytoscape: a software environment for integrated models of biomolecular interaction networks. *Genome Res* **13**: 2498-2504.

Smith, J.J., Marelli, M., Christmas, R.H., Vizeacoumar, F.J., Dilworth, D.J., Ideker, T., Galitski, T., Dimitrov, K., Rachubinski, R.A., and Aitchison, J.D. 2002. Transcriptome profiling to identify genes involved in peroxisome assembly and function. *J Cell Biol* **158**: 259-271.

Sokal, R.R. and Rohlf, F.J. 1995. *Biometry*. W. H. Freeman and Company.

Steffen, M., Petti, A., Aach, J., D'Haeseleer, P., and Church, G. 2002. Automated modelling of signal transduction networks. *BMC Bioinformatics* **3**: 34.

Veenhuis, M., Mateblowski, M., Kunau, W.H., and Harder, W. 1987. Proliferation of microbodies in Saccharomyces cerevisiae. *Yeast* **3**: 77-84.

SUPPLEMENTAL WEBSITE REFERENCES

http://mips.gsf.de , Munich Information Center for Protein Sequences (MIPS)

http://www.bind.ca , Biomolecular Interaction Network Database (BIND)

http://www.cytoscape.org , Cytoscape homepage

http://labs.systemsbiology.net/galitski , Galitski Lab homepage

http://java.sun.com , Sun Microsystems Java Technology Source page